

# THERMAL INTERACTION OF CRYOGEN SPRAY WITH HUMAN SKIN UNDER VACUUM PRESSURES

Walfre Franco<sup>1</sup>, Jorge Perez<sup>1</sup>, Jie Liu<sup>1</sup>, Guillermo Aguilar<sup>1</sup>  
<sup>1</sup>Department of Mechanical Engineering, University of California Riverside,  
Riverside, CA, 92521, USA. [gaguilar@engr.ucr.edu](mailto:gaguilar@engr.ucr.edu)

**Abstract.** *Clinical results of port wine stain (PWS) birthmarks laser therapy have shown that dark purple lesions usually respond well to the first 3–5 treatments. However, for most PWS, complete blanching is never achieved, and the lesion stabilizes at a red-pink color. We have recently demonstrated that with the aid of a local vacuum applied to the lesion site prior to laser irradiation, photocoagulation of the smaller vessels in PWS birthmarks can be successfully achieved. We have then hypothesized that the release of cryogen spurts under vacuum pressures may also offer many advantages to this therapeutic procedure due to different spray-surface interactions under vacuum conditions. The objective of our work is to study the thermal response of a skin phantom to CSC at vacuum pressures. For this purpose, liquid cryogen was sprayed onto a skin phantom under atmospheric and various vacuum pressures, ranging from -17 to -70 kPa, at two nozzle-surface distances, 30 and 40 mm. We used a temperature sensor mounted on the phantom surface to measure temperature changes as a function of time, and an analytical solution, based on Fourier's law and Duhamel's theorem, to calculate heat flux and overall heat removal. Compared to atmospheric pressures, lower minimum surface temperatures and higher heat removal from the skin phantom were observed under all vacuum pressures and both surface-nozzle distances used in this study. This approach enhances the heat extraction from the skin surface and, therefore, should help improving epidermal protection provided by CSC during PWS laser therapy.*

**Keywords:** *vacuum pressure, laser therapy, cryogen spray cooling, vascular lesions*

## 1. INTRODUCTION

During the treatment of port wine stain (PWS) birthmarks laser energy is irradiated at appropriate wavelengths to photocoagulate undesired blood vessels embedded in the dermis. An important limitation of this procedure is that laser energy is also absorbed by epidermal melanin, causing localized heating therein. To overcome this limitation, cryogen spray cooling (CSC) is used to lower selectively the temperature of the epidermis (Anvari, *et al.*, 1995, Nelson, *et al.*, 1995, Paithankar, *et al.*, 2002). Despite the widespread use of CSC-assisted skin laser treatments, clinical studies have demonstrated that dark purple PWS respond well to the first 3–5 treatments with improved lesion blanching. Thereafter, lesion color stabilizes at a red-pink color showing a poor response to further treatments. This response may be due to the difficulty in destroying small vessels because the ratio of blood to total volume (blood, vessel wall and perivascular tissue) is too small (vanGemert, *et al.*, 1997). It follows that the thermal confinement required to reach the threshold for permanent vessel damage is insufficient (Svaasand, *et al.*, 1995).

Table 1. Thermal properties of epidermis and sensor materials

	epidermis	epoxy	silver foil
$c$ (J/kg K)	3600	—	235
$\rho$ (kg/m <sup>3</sup> )	1200	1160-1400	10500
$k$ (W/m K)	0.21	0.217	429
$\alpha$ (m <sup>2</sup> /s)	$0.5 \times 10^{-7}$	$1.2 \times 10^{-7}$	$1739 \times 10^{-7}$

Recent clinical studies propose increasing the volumetric blood fraction to enlarge small blood vessels such that sufficient thermal confinement to photocoagulate them can be achieved. (Svaasand *et al.*, 2004) used a pressure cuff to obstruct venous return in the proximal arm to increase the blood flow in the distal upper extremity; 40% less radiant exposure was required to induce the same amount of purpura as compared to the case without pressure cuff. Aguilar *et al.* (2005b) applied local vacuum on the lesion site to increase the blood flow; 35% less laser fluence was required to induce the same amount of purpura as compared to the atmospheric conditions case, and blanching was clinically significant for most sites treated under partial vacuum conditions. The first study about implications of partial vacuum pressures on CSC was done by Aguilar *et al.* (2005a). Under atmospheric and partial vacuum conditions, the authors used: video analysis to show that cryogen spurts do not produce skin indentation and only minimal frost formation; image analysis to show that shorter jet lengths and better spray atomization occurs and skin phantoms to show that lower minimum surface temperatures and higher heat removal are reached. In the present study the thermal response to CSC produced by a nozzle at two surface-nozzle distances under atmospheric and four vacuum pressures is investigated.

## 2. EXPERIMENTAL AND NUMERICAL METHODS

### 2.1 Spray Cooling System

Refrigerant hydrofluorocarbon 134a (Suva® 134a, Dupont) is delivered through a high pressure hose to an electronic valve (Series 99, Parker Hannifin Corp., Cleveland OH) attached to a straight-tube nozzle with 32 mm length and 0.5 mm inner diameter (0.02 in, Small Parts Inc., Miami Lakes FL). R134a has a boiling temperature at atmospheric pressure of  $\approx -26$  °C and is kept in its original container at a pressure of 600 kPa and room temperature of 22 °C. The spray system is set to deliver 100 ms spurts 30 and 40 mm away from the thermal sensor surface.

### 2.2 Thermal Sensor and Skin Phantom

The thermal sensor consists of a type-K thermocouple (CHAL-005, Omega, Stamford CT) soldered to a silver foil ( $\approx 3 \times 3$  mm surface and  $L \approx 0.09$  mm thickness) embedded in an epoxy resin (RBC 3100, RBC, Warwick RI). The sensor employed, similar to those reported previously (Basinger, *et al.*, 2004), provides a substrate with thermal properties similar to human skin. The standard error limit of type-K thermocouples is 2.2 °C or 2%. Specific heat  $c$ , density  $\rho$ , thermal conductivity  $k$  and thermal diffusivity  $\alpha$  of epidermis, epoxy and silver foil are presented in Table 1. Temperature is acquired through National Instruments hardware (NI PCI-6111 S Series Multifunction) and software (LabView 7) at

4000 Hz. Noise is filtered out using a running average of previous and next 15 points. The initial temperature of the thermal sensor before any spurt is 22 °C for all experiments.

### 2.3 Vacuum Pressure Chamber

A 300×380 mm cylindrical vacuum chamber (Terra Universal Inc., Anaheim CA) made of acrylic is used to enclose the spray system, thermal sensor and skin phantom. The chamber pressure is lowered by a vacuum pump to carry out experiments at 0, 16.9, 33.9, 50.8 and 67.7 kPa (0, 5, 10, 15 and 20 in Hg) vacuum pressures. Saturation temperatures of liquid cryogen at these pressures are shown in Table 2.

Table 2. Saturation temperatures of R134a at specific vacuum pressures

$P$ (kPa) [in Hg]	$P_{abs}$ (kPa)	$\approx T_{sat}$ (°C)
0	101.3	-26
16.9 [5]	84.4	-30
33.9 [10]	67.4	-35
50.8 [15]	50.5	-40
67.7 [20]	33.6	-48

### 2.4 Heat flux calculations

Duhamel's theorem states that the substrate thermal response at  $t$  equals the total sum of what the substrate experienced in small steps prior to  $t$ . Assuming constant thermal properties, Duhamel's theorem can be written as

$$\theta(z, t) = \theta_o + \int_{t_o}^t u(z, t - \tau) \frac{dT}{d\tau} d\tau, \quad (1)$$

where  $z$  is the coordinate perpendicular to the surface,  $T$  is the surface temperature,  $\theta$  is the substrate temperature,  $\theta_o$  is the uniform initial temperature,  $u$  is the temperature response function of the substrate (initially at zero temperature) to a unit step in surface temperature, and  $t-\tau$  is the time that has elapsed since the step at  $\tau$ . The unit step function for a semi-infinite planar solid is

$$u(z, t) = 1 - \operatorname{erf}\left(\frac{z}{2\sqrt{\alpha t}}\right). \quad (2)$$

Substituting Eq. 1 and 2 into Fourier's law gives

$$q(t) = \sqrt{\frac{k\rho c}{\pi}} \int_{t_o}^t \frac{1}{\sqrt{t-\tau}} \frac{dT}{d\tau} d\tau, \quad (3)$$

which can be integrated analytically to calculate the approximate surface heat flux  $\bar{q}$  in a semi-infinite planar body with discrete surface temperature measurements  $T_i$  at time  $t_i$  as

$$\bar{q}(t_I) = 2\sqrt{\frac{k\rho c}{\pi}} \sum_{i=1}^I \frac{T_i - T_{i-1}}{\sqrt{t_I - t_i} + \sqrt{t_I - t_{i-1}}}. \quad (4)$$

Equation 4 is used to calculate the surface heat flux and integrated over time to compute the total heat removal  $Q$ . For simplicity,  $\bar{q}$  is written as  $q$  in the next sections. A more detailed derivation of Eq. 4 can be found in Franco, *et al.*, (2005).

### 3. RESULTS AND DISCUSSION

Although spray-skin phantom thermal interactions at five different pressures are investigated, dynamics of surface temperature  $T$ , heat flux  $q$  and heat removal  $Q$  are presented only for vacuum pressure  $P=0, 33.9$  and  $67.7$  kPa (0, 10 and 20 in Hg) and surface-nozzle distances of  $z=30$  and  $40$  mm. However, characteristic values of heat transfer, such as minimum surface temperature  $T_{min}$  and maximum surface heat flux  $q_{max}$ , are shown for every  $P$  and  $z$ .

#### 3.1. Dynamics of surface temperature

The temperature response of the skin phantom to 100 ms cryogen spurts released at atmospheric, 33.9 and 67.7 kPa vacuum pressures is presented in Figs. 1a and 1b for nozzle-to-surface distances of 30 and 40 mm, respectively. Note that CSC imposes different thermal dynamics quantitatively and qualitatively at each  $z$  and  $P$ . The horizontal dashed lines in each subfigure represent saturation temperatures  $T_{sat}$  at specific pressures (see Table 2). In Fig. 1(a) it is observed that  $T$  drops to  $\approx -35$  °C and then increases to  $T_{sat} \approx -26$  °C for  $P=0$  kPa and remains at this temperature for a significant amount of time ( $\approx 1500$  ms); consequently, liquid cryogen may accumulate on the skin phantom surface while  $T < T_{sat}$  and evaporate while  $T = T_{sat}$ . At  $P=33.9$  kPa,  $T$  drops to  $\approx -40$  °C and then increases past  $T_{sat}$ ; it follows that an accumulation of liquid seems to be less likely to occur. At  $P=66.7$  kPa,  $T$  drops to  $\approx -50$  °C and barely reaches  $T_{sat}$ ; thus, there is no accumulation of liquid cryogen. The plateau at 0 °C corresponds to the local water vapor that condenses on the phantom surface and freezes. In Fig. 1(b) it is observed that  $T$  drops to  $T_{sat}$  at 0 kPa while never reaches  $T_{sat}$  at 33.9 and 66.7 kPa since fewer droplets reach the surface compared to  $z=30$  mm because of a better evaporation.

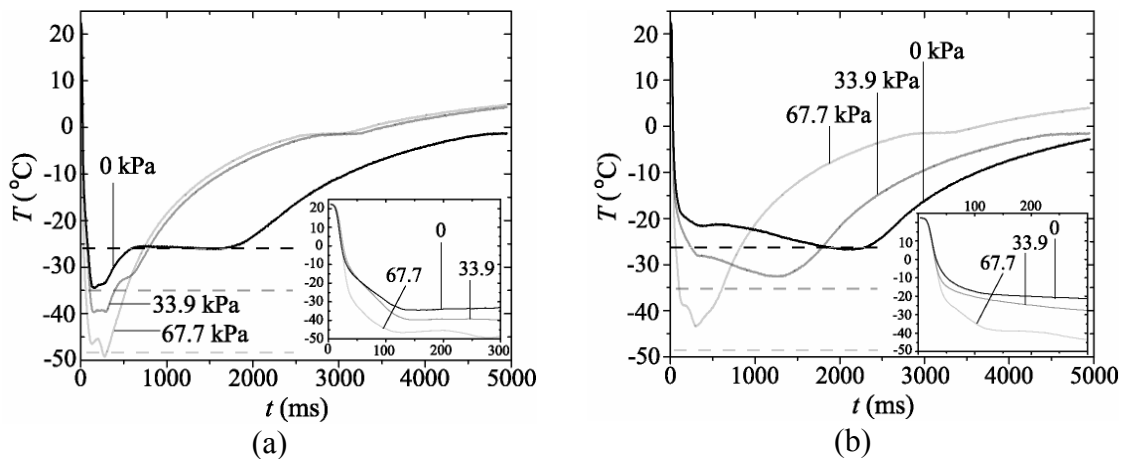


**Figure 1.** Temperature response of skin phantom to liquid cryogen sprayed at atmospheric and vacuum pressures at (a)  $z = 30$  and (b)  $z = 40$  mm from the surface.

#### 3.2. Dynamics of surface heat flux

The heat flux response of the skin phantom to 100 ms cryogen spurts 30 and 40 mm away from the surface is shown in Fig. 2 for atmospheric (0), 33.9 and 67.7 kPa vacuum pressures.  $q(t)$  is shown for the first 300 ms (when most of the heat extraction occurs),

thereafter there is a slow decay in magnitudes. At  $z=30$  mm, Fig. 2(a), the highest  $q(t)$  along the 300 ms period shown takes place at  $P=66.7$  kPa. At  $z = 40$  mm, Fig. 2(b), higher  $q$  corresponds to the higher vacuum pressure ( $P$ ). Note that the maximum on each curve occurs before the spray ends and that the time of occurrence increases as  $P$  increases.

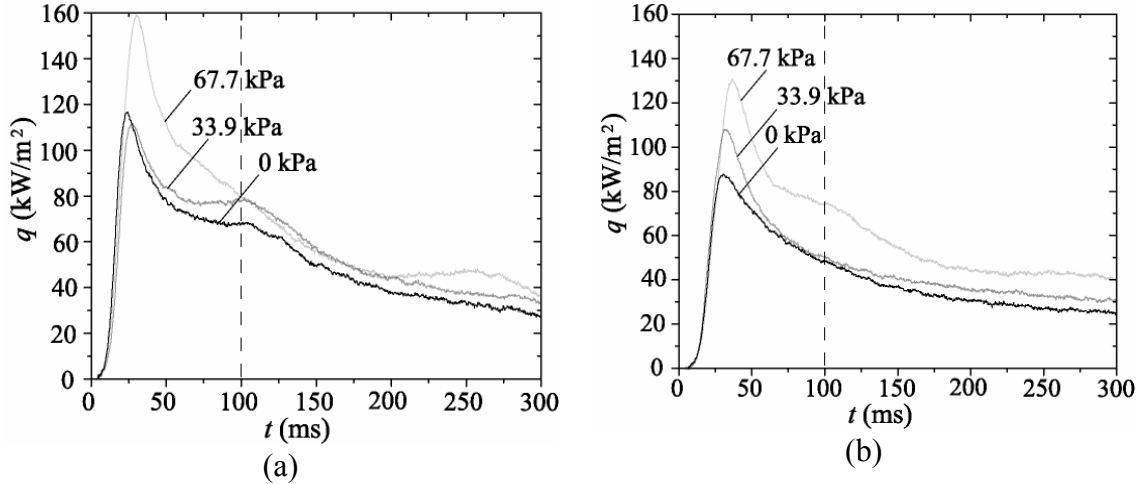


**Figure 2.** Heat flux response of skin phantom to liquid cryogen sprayed at atmospheric and vacuum pressures at (a)  $z = 30$  mm and (b)  $z = 40$  mm from the surface.

### 3.3. Total heat extraction

The total heat removal from the skin phantom  $Q(t)$  by cryogen spray cooling at atmospheric, 33.9 and 67.7 kPa vacuum pressures is shown in Figs. 3a and 3b for  $z = 30$  and 40 mm, respectively.  $Q(t)$  is also shown for the first 300 ms, when most of the heat is removed from the skin phantom. Fig. 3(a) shows that the highest  $Q$  occurs at  $P=67.7$  kPa and there is not a significant difference in  $Q$  between  $P=0$  and 33.9 kPa during the first 150 ms. For  $z = 40$  mm, Fig. 3(b), it is clear that the higher  $P$  is the higher  $Q$  is. Although  $q$  is a more important safety parameter for therapies in which cooling selectivity of the upper skin layer is critical (e.g. PWS laser surgery),  $Q$  is more important to assess the cooling protection for therapies where deeper structures (e.g., hair follicles) are targeted and for which the time in which the heat is extracted is not as critical at the amount.

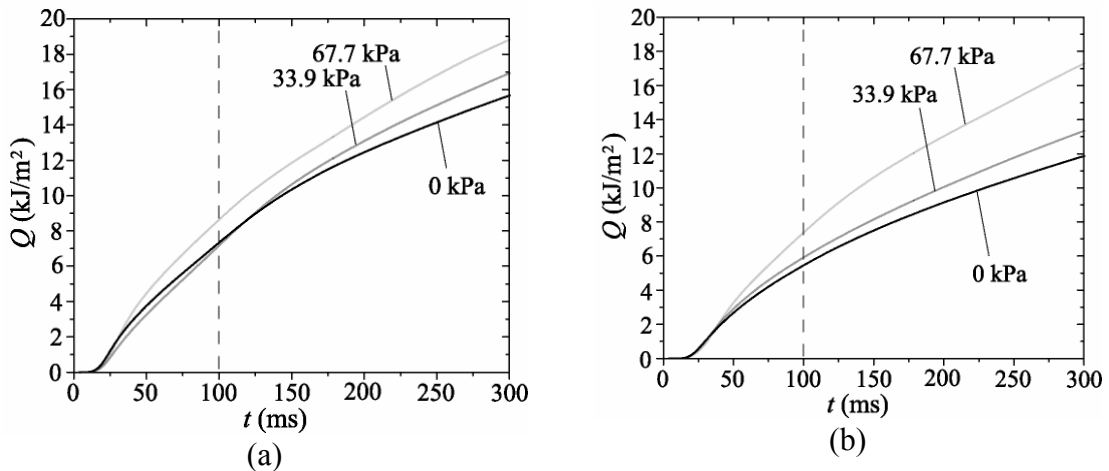


**Figure 3.** Heat removal from skin phantom by liquid cryogen sprayed at atmospheric and vacuum pressures at (a)  $z = 30$  mm and (b)  $z = 40$  mm from the surface.

### 3.4. Effects on characteristic values

Figure 4(a) shows  $T_{min}$  as a function of  $P$ , that is, lower surface temperatures are reached at higher vacuum pressures (lower absolute pressures). Figure 4(b) shows  $q_{max}$  as a function of  $P$ , where the trend seems to be that higher maximum heat fluxes occur at higher vacuum pressures, except for the fact that  $q_{max}$  at 0 kPa is higher or as high as that at 33.9 kPa. Lower pressures impose a larger cryogen expansion (from 600 kPa in the container to vacuum chamber pressure) which translates into higher shear stresses and, consequently, into better liquid atomization that enhances droplet evaporation. These variations imply a change in the size and velocity of droplets impinging on the skin phantom surface. Cryogen droplets may become smaller as pressure lowers and take longer to wet the surface. Fig. 2 shows that the lower the absolute pressure is, the later  $q_{max}$  occurs. Therefore, when the nozzle is placed at short distances from the phantom, e.g.,  $z = 30$  mm, small changes in pressure have a small effect on the surface heat flux.

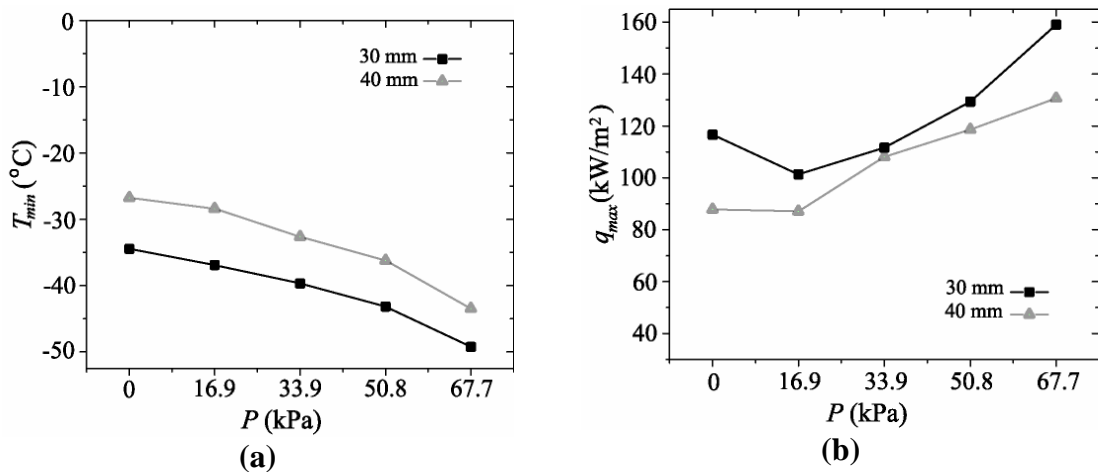


**Figure 4.** (a) Minimum temperature and (b) maximum heat flux as a function of pressure and surface-nozzle distance.

The minimum seen in Fig. 4b for  $z = 30$  mm is likely to be the effect of two competing phenomena, one of which dominates at low vacuum pressures but is overcome by the other as vacuum pressure increases. As the spray is released into the vacuum pressure chamber, a larger adiabatic expansion takes place compared to that at atmospheric pressure. The larger pressure differential increases the average in-flight and impact velocities of droplets, while it also induces a higher evaporation rate and, therefore, the average droplet temperature diminishes. Both of these phenomena combined would lead, in principle, to a higher heat flux. However, a higher evaporation rate would also reduce the average droplet size and diminish the number of droplets that reach the surface. The latter two effects would have a counteracting effect on the heat flux. The results obtained would seem to suggest that at low vacuum pressures (16.9 kPa) the reduction in droplet size and number dominate the effects on  $q_{max}$ , while at higher vacuum pressures, the further increase in droplet impact velocity and decrease in average droplet temperature are more pronounced and, therefore, lead to higher  $q_{max}$ .

## 4. CONCLUSIONS

This work focused on measuring the overall effect of vacuum pressures on the heat extraction from human skin phantoms during cryogen spray cooling (CSC). Higher surface heat fluxes with respect to atmospheric conditions take place for  $P > 33.9$  kPa (10 in Hg) at  $z = 30$  mm and  $P > 16.9$  kPa (5 in Hg) at  $z = 40$  mm. For both cases, however, CSC under vacuum pressures enhances the heat extraction from the skin surface compared to that measured at atmospheric pressure. These results alone should help improving epidermal protection provided by CSC during PWS laser therapy. The enhanced heat extraction measured in these experiments is a consequence of the effect that vacuum pressures have on the atomization and evaporation dynamics of cryogen spray droplets, which may be observed as variations in the spray droplet size, velocity and temperature distributions with respect to those at atmospheric pressure. Our ongoing work is focused on establishing the relationship between these spray property variations and the overall heat extraction resulting from spraying cryogen sprays under vacuum pressures.

## ACKNOWLEDGEMENTS

This work was supported in part by the National Institutes of Health (HD42057), the American Society for Lasers in Surgery and Medicine (A. Ward Ford Memorial Institute Grant 2004-2005) and the Regents Faculty Fellowship (UCR).

## REFERENCES

- Aguilar, G., Franco, W., Liu, J., Svaasand, L. O. y Nelson, J. S., 2005a, "Effects of hypobaric pressure on human skin: Implications for cryogen spray cooling (Part II)". *Lasers Surg Med*, 36: pp. 130-135.
- Aguilar, G., Svaasand, L. O. y Nelson, J. S., 2005b, "Effects of hypobaric pressure on human skin: Feasibility study for port wine stain laser therapy (Part I)". *Lasers Surg Med*, 36: pp. 124-129.
- Anvari, B., Tanenbaum, B. S., Milner, T. E., Kimel, S., Svaasand, L. O. y Nelson, J. S., 1995, "A theoretical study of the thermal response of skin to cryogen spray cooling and pulsed laser irradiation: implications for treatment of port wine stain birthmarks". *Phys Med Biol*, 40: pp. 1451-1465.
- Basinger, B., Aguilar, G. y Nelson, J. S., 2004, "Effect of skin indentation on heat transfer during cryogen spray cooling". *Lasers in Surgery and Medicine*, 34: pp. 155-163.
- Franco, W., Liu, J., Wang, G. X., Nelson, J. S. y Aguilar, G., 2005, "Radial and temporal variations in surface heat transfer during cryogen spray cooling". *Physics in Medicine and Biology*, 50: pp. 387--397.
- Nelson, J. S., Milner, T. E., Anvari, B., Tanenbaum, B. S., Kimel, S., Svaasand, L. O. y Jacques, S. L., 1995, "Dynamic Epidermal Cooling During Pulsed-Laser Treatment of Port-Wine Stain - a New Methodology with Preliminary Clinical-Evaluation". *Archives of Dermatology*, 131: pp. 695-700.
- Paithankar, D. Y., Ross, E. V., Saleh, B. A., Blair, M. A. y Graham, B. S., 2002, "Acne treatment with a 1,450 nm wavelength laser and cryogen spray cooling". *Lasers Surg Med*, 31: pp. 106-114.
- Svaasand, L. O., Aguilar, G., Viator, J. A., Randeberg, L. L., Kimel, S. y Nelson, J. S., 2004, "Increase of dermal blood volume fraction reduces the threshold for laser-induced purpura: Implications for port wine stain laser treatment". *Lasers in Surgery and Medicine*, 34: pp. 182-188.

- Svaasand, L. O., Fiskerstrand, E. J., Kopstad, G., Norvang, L. T., Svaasand, E. K., Nelson, J. S. y Berns, M. W., 1995, "Therapeutic response during pulsed laser treatment of port-wine stains: Dependence on vessel diameter and depth in dermis". *Lasers in Medical Science*, 10: pp. 235-243.
- vanGemert, M. J. C., Smithies, D. J., Verkruysse, W., Milner, T. E. y Nelson, J. S., 1997, "Wavelengths for port wine stain laser treatment: Influence of vessel radius and skin anatomy". *Phys Med Biol*, 42: pp. 41-50.